URSI-RCRS 2024, ARIES/GEHU, Bhimtal, India, 22 - 25 October, 2024

Magnetic Field based Satellite Attitude Estimation and Safe Mode Detection

Shashank Tomar(1), Kanu Priya Govila (1), and Shubha Kapoor(1)
(1) U.R. Rao Satellite Centre, Bengaluru, India

Abstract

Ensuring accurate spacecraft attitude determination is paramount for the success of contemporary space missions, particularly with the ongoing trend of miniaturization and standardization of satellites to optimize launch costs and manage constellations efficiently. This paper addresses the pressing demand for cost-effective and resource-efficient attitude determination methods in this evolving landscape. The paper builds on the methodology of the two-step Kalman Filter, first proposed in [1], to create an estimator that uses on-board magnetic field measurements and IGRF model based magnetic field data for satellite attitude and rate determination. The developed estimator works for a wide range of satellite angular velocities, is robust to uncertainties in Magnetic field measurement, satellite inertia, disturbance torques and satellite state (position and velocity). The resulting filter emerges as a viable primary attitude determination solution for small satellites or as an independent backup estimator in traditional satellites. The paper also introduces a novel application of the developed estimator to trigger safe mode, ensuring the safety and efficacy of emergency operations.

1. Introduction

Accurate spacecraft attitude determination is crucial for successful space missions, impacting navigation, communication, and scientific observations. The prevalent method combines star trackers and gyroscopes for determining attitude and angular rate, which is accurate and reliable but bulky, space-consuming, and power-intensive. With the rise of nano and microsatellite missions favoring multiple small satellites, there is a need for low-mass, volume, and power-efficient attitude determination methods, especially for small satellite missions with moderate pointing accuracy requirements. Magnetometers, already onboard most satellites for momentum dumping via magnetorquers, are highly reliable and efficient in terms of power consumption, mass, and volume.

The problem of gyroless attitude determination has been extensively studied. Early methods employed vector-based determination to calculate direction cosines, such as the TRIAD, QUEST, and Wahba's method[2]. Natanson et al.'s DADMOD method [3] used magnetic field measurements, their derivatives, and angular acceleration knowledge for attitude and rate estimation. The most popular methods, employing Extended Kalman Filters (EKFs), have shown varying degrees of accuracy. Psiaki's Kalman filtering demonstrated errors of around 2–3 degrees after 100 seconds with low initial uncertainty [4]. Searcy and Pernicka's two-step EKF algorithm achieved attitude errors of less than 1 degree but failed if initial angular rates exceeded 0.1°/s[1]. Ma and Jiang proposed an Unscented Kalman Filter (UKF) based algorithm, but it is computationally inefficient for satellite systems [5]. Wattanarungsan et al.[6] improved reliability and convergence time by resolving singularity in the estimator using optimization techniques. Crassidis et al.[7] explored onboard magnetometer calibration methods.

However, existing methods do not fully address key concerns in satellite control design:

1) Uncertainty in Moment of Inertia knowledge
2) Magnetometer measurement variance and bias
3) Uncertainty in Satellite position and velocity
4) Very low initial angular velocities (~0.06 deg/s)

The proposed estimation strategy in this paper is robust to these variations. Additionally, it suggests using the developed estimator as a safe mode trigger. In scenarios where the gyro fails or provides faulty measurements, the proposed innovation vector-based safe mode detection acts as an additional safety layer.

3. Problem Formulation

The magnetometer-based attitude determination problem boils down to solving for the rotation angles (spacecraft attitude) that transforms the magnetic field in spacecraft frame (B_b) to that in the inertial frame (B_i). However, in order to uniquely solve for the rotation, we need one additional vector in each frame. These are the derivatives of the magnetic field in body frame ($\dot{B}_b$) and inertial frame($\dot{B}_i$). The resulting equations are as follows [1]

$$\langle 0, B_b \rangle = q^c \langle 0, B_i \rangle \tag{1}$$

$$\langle 0, \dot{B}_b \rangle = \dot{q}^c \langle 0, B_i \rangle q + q^c \langle 0, \dot{B}_i \rangle q + q^c \langle 0, B_i \rangle \dot{q} \tag{2}$$

Here q is the spacecraft attitude quaternion, and q^c is the conjugate. The "vector" part of the quaternion are the last three elements and the first element is the "scalar" part. Notice that equations (1) and (2) on simplification yield only 6 equations for 8 variables (q and $\dot{q}$). Equations (3) and (4) are the constraint equations that result in 8 equations for 8 variables:

$$\|q\| = 1 \text{ i.e. } q_0^2 + q_1^2 + q_2^2 + q_3^2 = 1 \tag{3}$$

$$2\dot{q}_0\,\dot{q}_0 + 2\dot{q}_1\,\dot{q}_1 + 2\dot{q}_2\,\dot{q}_2 + 2\dot{q}_3\,\dot{q}_3 = 0 \tag{4}$$

The spacecraft angular velocity can be computed as $q^* = \frac{1}{2} q w^*$, where $w^* = \langle 0, \omega \rangle$ is the quaternion representation of the angular velocity ω. Equations (1-4) can in principle be solved directly for the spacecraft attitude and rate. However, these equations are highly non-linear and solving them on-board in real time is not feasible.

4. Solution Methodology

The solution methodology has two steps. The first is to compute $\dot{B}_b$ and $\dot{B}_i$ by filtering B_b (measured with an onboard magnetometer) and B_i. B_i is computed using the International Geomagnetic Reference Field (IGRF) model. This pre-filtering process to estimate the Magnetic field derivative is done with a Kalman filter using a third-order Markov process to model the magnetic field, given by [1]:

$$\frac{dB}{dt} = \dot{B} \quad \frac{d\dot{B}}{dt} = \ddot{B} \quad \frac{d\ddot{B}}{dt} = 0 \tag{5}$$

These equations can be used to derive the first Kalman filter. A brief description of Kalman filters is provided below, interested readers are referred to [8]. Consider

$$\begin{aligned} \dot{x} &= f(x) + u \\ y &= h(x) + v \end{aligned} \tag{6}$$

Where x is the state of the system, y is the measurement, u is the process noise with covariance Q and v is the measurement noise with covariance R. The system and measurement Jacobian matrices F and H are defined as:

$$F = \frac{\partial f(x)}{\partial x} \; H = \frac{\partial h(x)}{\partial x} \tag{7}$$

The system dynamics are propagated in time using equation (6), whereas the error is propagated using the covariance propagation equation, given by:

$$\dot{P} = FP + PF^T + Q \tag{8}$$

Where P is the estimate error covariance. The result of the system dynamics propagation is known as the apriori estimate, designated by a "bar" ($\underline{x}$). The Kalman Filter fuses the measurement information with the apriori estimate to yield the posteriori estimate, designated by a "caret" ($\hat{x}$). The equations for the same are as follows:

$$K_k = \underline{P}_k H_k^T \left(H_k \underline{P}_k H_k^T + R_k \right)^{-1} \tag{9}$$

$$\hat{x}_k = \underline{x}_k + K_k(y_k - h_k(\underline{x}_k)) \tag{10}$$

$$\hat{P}_k = (I - K_k H_k)\underline{P}_k \tag{11}$$

Equation (5) represents the system dynamics of the pre-filter (used to estimate magnetic field derivatives). The state dynamics can be written in state space form as:

$$\dot{x} = \frac{d}{dt}\left[B_x \; B_y \; B_z \; \dot{B}_x \; \dot{B}_y \; \dot{B}_z \; \ddot{B}_x \; \ddot{B}_y \; \ddot{B}_z \;\right]^T \tag{12}$$
$$= \left[\dot{B}_x \; \dot{B}_y \; \dot{B}_z \; \ddot{B}_x \; \ddot{B}_y \; \ddot{B}_z \; 0 \; 0 \; 0\right]^T$$

The measurement y is

$$y = \left[B_x \; B_y \; B_z \;\right]^T \tag{13}$$

The state and measurement Jacobian matrix (F and H) can be directly computed [1].
The second Kalman Filter takes the filtered states (B_b,B_i, $\dot{B}_b$,$\dot{B}_i$) and uses it to estimate the satellite attitude and rate (q, ω). The measurements for this filter are:

$$y = \left[B_{b_x} \; B_{b_y} \; B_{b_z} \; \dot{B}_{b_x} \; \dot{B}_{b_y} \; \dot{B}_{b_z} \;\right]^T \tag{14}$$

The system dynamics consists of the quaternion derivative and Euler's rigid body equations of motion, given by:

$$\begin{aligned} \dot{x} &= \frac{d}{dt}\left[q_0 \; q_1 \; q_2 \; q_3 \; \omega_x \; \omega_y \; \omega_z \;\right]^T = \\ &= \left[\frac{1}{2} q\omega^* \quad [J]^{-1}(T - \omega \times ([J]\omega)) \;\right] \end{aligned} \tag{15}$$

Where T is net external torque acting on the spacecraft and *[J]* is the satellite's moment of inertia. The matrix F for the second Kalman filter can be computed by taking the Jacobian of equation (15). Similarly, the matrix H be computed by taking the Jacobian of the following equation:

$$y = \left[q^c \langle 0, B_i \rangle q \;\; \frac{1}{2} q\omega^* \langle 0, B_i \rangle q + q^c \langle 0, \dot{B}_i \rangle q + q^c \langle 0, B_i \rangle \frac{1}{2} q\omega^* \;\right] \tag{16}$$

For brevity's sake, the complete analytic expressions for the computed F and H matrices are not written here.
The implementation of the pre-filter in the current work is identical to [1]. The second filter however has the following changes which lead to higher accuracy and robustness compared to the implementation in [1]

1) Use of the complete inertia matrix, instead of only the diagonal terms as in [1]. Including the off-diagonal terms decreased state estimation error.
2) Computing analytic Jacobian matrix H instead of finite-differencing the measurements as in [1].
3) Using the Joseph stabilized version of the covariance measurement update (equation (10)). This guarantees that the covariance matrix $\hat{P}_k$ will always be symmetric positive definite, leading to stable and robust implementation [8].

The Joseph stabilized version of the covariance measurement update is given by [12]:

$$\hat{P}_k = (I - K_k H_k)\underline{P}_k \left(I_{K_k H_k}\right)^T + K_k R_k K_k^T \tag{17}$$

4. Results

4.1 Simulation Conditions

In order to demonstrate the efficacy of the developed estimator, two initial conditions are chosen for the satellite. A lower initial angular velocity of [0,0,-0.06] degree/s (inertial rate for typical satellites) and a high initial angular velocity of [5,-5,5] deg/s. There is no net external torque acting on the body (to evaluate estimator performance). The satellite is assumed to be in 450 km circular orbit around earth, at an inclination of 45 degrees. The inertial magnetic field readings are generated from the IGRF 2015 model. The satellite moment of inertia is taken to be

$$[J] = [1200 \; -20 \;\; 20 \;\; -20 \;\; 1050 - 25 \;\; 20 \; - 25 \;\;\; 1360 \;] kg \; m^2 \tag{18}$$

The following uncertainties were included in simulations:
1) 10% uncertainty in Inertia
2) Magnetometer measurement: 500 gamma noise, 100 gamma uncorrected bias
3) Satellite position (15 m) and velocity (0.15 m/s)

Note that uncertainty in satellite position leads to uncertainty in B_i and consequently in B_b which leads to increased error in the estimated satellite position and rate

4.2 Pre-filter results

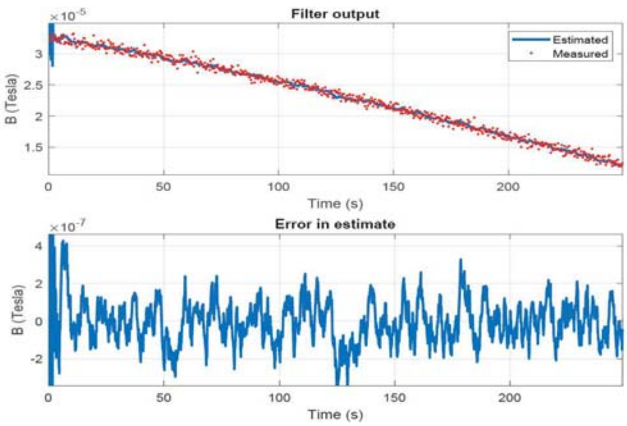

Figure 1. Variation of Measured magnetic field against the estimated field for lower initial angular velocity

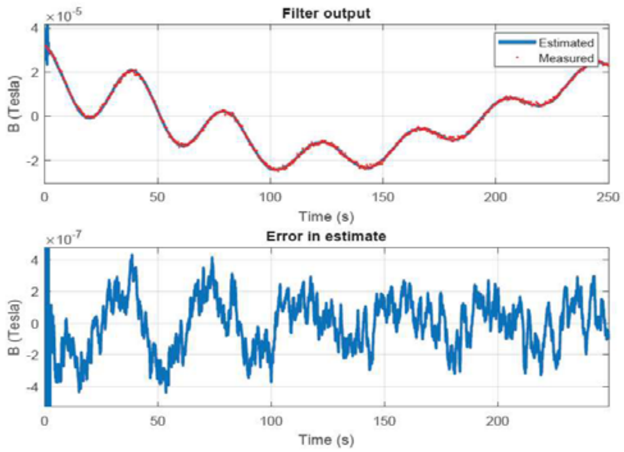

Figure 2. Variation of Measured magnetic field against the estimated field for higher initial angular velocity

The filtered magnetic field for lower and higher initial angular velocities can be seen in Figures [1] and [2]. For clarity, only single axis data are plotted here.We see that the filter converges very quickly (less than 10 seconds) and the estimated magnetic field closely follows the measured data, while reducing the noise and error. The error band in the filtered output for lower initial rate (Figure [1]) is 3e-7 Tesla (300 Gamma) which is lower than the measurement noise. Even for the higher initial rate (Figure [2]) the error band in the filtered measurement is 5e-7 (500 Gamma) which is of the same order as the measurement noise due to the oscillations in magnetometer readings introduced by the high satellite spin.

4.2 Attitude and Rate Estimation Results

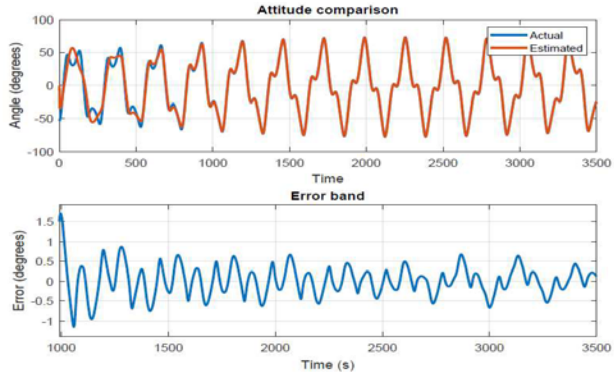

Figure 3. Error in Estimated spacecraft attitude compared to the true attitude for higher initial angular velocity

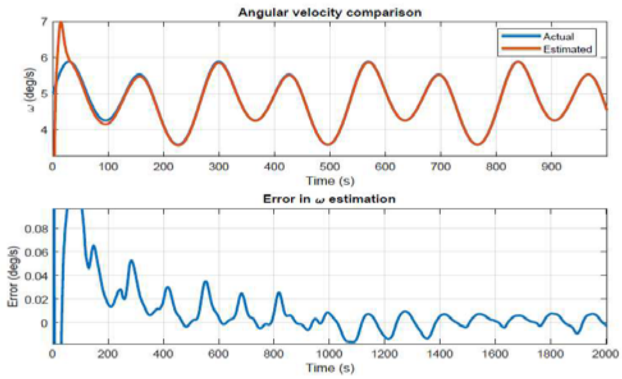

Figure 4. Error in Estimated spacecraft rate compared to the true rate for higher initial angular velocity

The satellite attitude and rate are estimated using the filtered measurements as input. For high initial angular velocity (Figure [3]), we see that the filter converges faster (within 1000 s). The error in attitude estimation is less than a degree, whereas the angular velocity is tracked within an error of 0.02 deg/s (Figure [4]).

For the lower initial angular velocity (Figures [5-6]) the convergence is slower and it takes nearly 4000 seconds before the attitude and rate are properly tracked. Physically, as a slowly rotating satellite will introduce smaller changes in the measured magnetic field, making attitude and rate determination difficult for the filter.

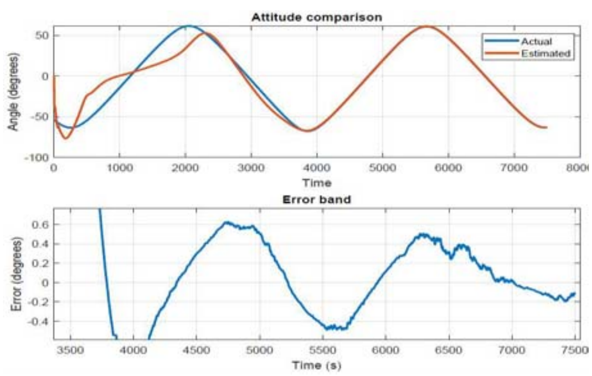

Figure 5. Error in Estimated spacecraft attitude compared to the true attitude for lower initial angular velocity

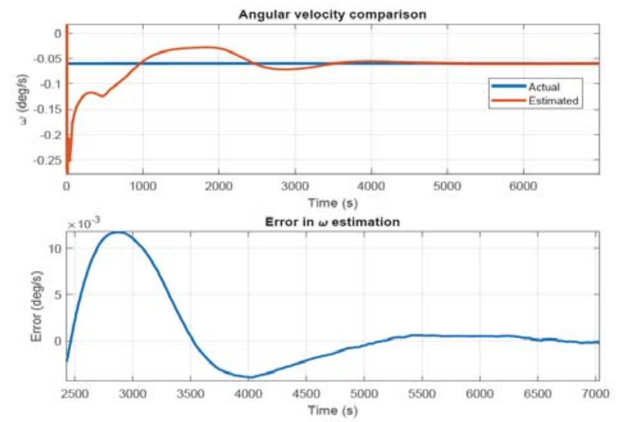

Figure 6. Error in Estimated spacecraft rate compared to the true rate for lower initial angular velocity

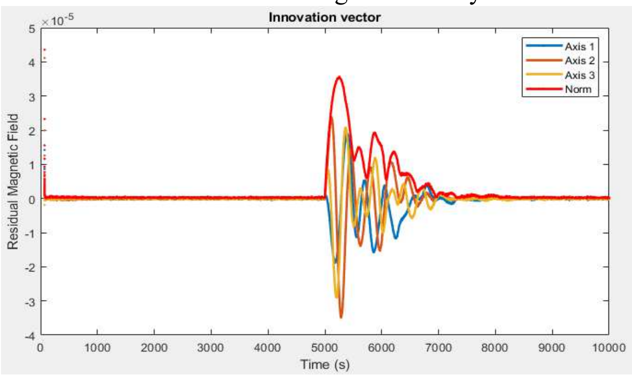

Figure 7. Innovation vector based safe mode detection. Disturbance rate of [0.5,-0.5,0.5] deg/s is injected at 5000 seconds post convergence.

However, contrary to the results in [1], our filter works better at lower initial rates, with an attitude error of less than 0.6 degrees and rates within 0.005 deg/s.

We also introduce a novel application of the Magnetometer based estimator as a safe mode trigger. Safe mode is triggered in satellites when the angular velocity exceeds a pre-set threshold. In traditional satellites, this is done by tracking the gyroscope rates. However, we propose to do this by detecting divergence in the innovation vector term of the second Kalman filter. From equation (10) the innovation vector is given by $y_k - h_k(\underline{x}_k)$ i.e the difference between the measured magnetic field and the estimated field. When the filter has converged, this takes on a very low value. We consider a case where a satellite moving with an initial angular velocity of [0 0 -0.06] deg/s is injected with a disturbance at 5000 s as seen in Figure [7]. We see an immediate and clear divergence in the innovation vector, which can be then used to trigger safe mode for the satellite. In this case, it detects divergence within 4 seconds. Future work would incorporate closed-loop simulations and torquer-magnetometer interactions.

5. Conclusions

A two-step Kalman filtering approach was employed to estimate satellite attitude and rate using noisy magnetometer readings and the IGRF model. The modeling details and improvements over previous work were highlighted. This approach includes a pre-filter for the magnetic field measurements and a second filter for estimating satellite attitudes and rates with high accuracy, even at very low rates. Notably, the estimator achieved errors of less than 0.6° in attitude and 0.005°/s in rate at low satellite angular velocities, which is a key novelty of this work. The filter was also robust to uncertainties in measurement, satellite position, velocity, and inertia. This makes it suitable as a backup estimator for traditional satellites or as the primary estimator for small satellite missions, where low power, mass, and volume are prioritized over high angular pointing accuracy. Additionally, a novel innovation-vector based safe mode detection algorithm was proposed, triggering a safe mode warning within 4 seconds. These advancements offer a practical solution to the challenges of spacecraft attitude determination, particularly for miniaturized satellites.

6. Acknowledgements

The authors would like to acknowledge and thank the support received at U.R. Rao Satellite Centre for the duration of the work.

7. References

1. Searcy, J.D.; Pernicka, H.J. Magnetometer-Only Attitude Determination Using Novel Two-Step Kalman Filter Approach.J. Guid. Control Dyn.**2012**,35,1639–1701.
2. Wahba, G., "A Least Squares Estimate of Satellite Attitude," SIAM Review, Vol. 7, No. 3, 1965, p. 409.
3. Natanson, M. S., Challa, G. A., Deutschmann, J., and Baker, D. F.,"Magnetometer-Only Attitude and Rate Estimation for Gyroless Spacecraft," Determination for a Gyroless Spacecraft," Proceedings of the Third International Symposium on Space Mission Operations and Ground Data Systems, NASA Conference Publication 3281, NASA-GSFC, Greenbelt, MD, Nov. 1994.
4. Psiaki, M., and Martel, F., "Three-Axis Attitude Determination via Kalman Filtering of Magnetometer Data," Journal of Guidance, Control, and Dynamics, Vol. 13, No. 3, 1990, pp. 506–514.
5. Ma, G., and Jiang, X., "Unscented Kalman Filter for Spacecraft Attitude Estimation and Calibration Using Magnetometer Measurements," Proceedings of the Fourth International Conference on Machine Learning and Cybernetics, Guangzhou, China, Aug. 2005.
6. S. Wattanarungsan, T. Kuwahara and S. Fujita, "Magnetometer-Based Attitude Determination Extended Kalman Filter and Optimization Techniques," in *IEEE Transactions on Aerospace and Electronic Systems*, vol. 59, no. 6, pp. 7993-8004, Dec. 2023
7. Crassidis, J. L., and Lai, K., "Real-Time Attitude-Independent Three-Axis Magnetometer Calibration," Journal of Guidance, Control, and Dynamics, Vol. 28, No. 1, 2005, pp. 115–120.
8. Simon, Dan., "Optimal State Estimation: Kalman, H_∞, and Nonlinear Approaches, John Wiley & Sons, Inc. 2006